Naval Research Laboratory

Washington, DC 20375-5320

NRL/MR/5710--98-8147

An Investigation of the Aerodynamic Performance of the Spin-Wing Concept

Steven K. Tayman
Andrea B. Walden

Off-Board Countermeasures Branch
Tactical Electronic Warfare Division

February 27, 1998

REPORT DOCUMENTATION PAGE

Form Approved
OMB No. 0704-0188

1. AGENCY USE ONLY *(Leave Blank)*	2. REPORT DATE	3. REPORT TYPE AND DATES COVERED
	February 27, 1998	Interim Report

4. TITLE AND SUBTITLE	5. FUNDING NUMBERS
An Investigation of Aerodynamics Performance of the Spin-Wing Concept	Work performed under NCRDAD-NRL-97-130
6. AUTHOR(S) Steven K. Tayman and Andrea B. Walden	
7. PERFORMING ORGANIZATION NAME(S) AND ADDRESS(ES) Naval Research Laboratory Washington, DC 20375-5320	8. PERFORMING ORGANIZATION REPORT NUMBER NRL/MR/5710--98-8147
9. SPONSORING/MONITORING AGENCY NAME(S) AND ADDRESS(ES) Office of Naval Research Arlington, VA 22217-5660	10. SPONSORING/MONITORING AGENCY REPORT NUMBER

11. SUPPLEMENTARY NOTES

12a. DISTRIBUTION/AVAILABILITY STATEMENT	12b. DISTRIBUTION CODE
Approved for public release; distribution unlimited.	

13. ABSTRACT *(Maximum 200 words)*

Unmanned air vehicles (UAV's) capable of vertical takeoff and landing (VTOL) are always of interest to the Navy. This paper examines the aerodynamic performance of a unique multi-mode aircraft concept called the spin-wing/stop rotor. The spin wing uses its wing and tail as a counter-rotating rotor system for hovering flight. For forward flight, the wing and tail are stopped.

14. SUBJECT TERMS	15. NUMBER OF PAGES
VTOL	17
	16. PRICE CODE

17. SECURITY CLASSIFICATION OF REPORT	18. SECURITY CLASSIFICATION OF THIS PAGE	19. SECURITY CLASSIFICATION OF ABSTRACT	20. LIMITATION OF ABSTRACT
UNCLASSIFIED	UNCLASSIFIED	UNCLASSIFIED	UL

NSN 7540-01-280-5500

Standard Form 298 (Rev. 2-89)
Prescribed by ANSI Std 239-18
298-102

TABLE OF CONTENTS

Preceding Page Blank

AN INVESTIGATION OF THE AERODYNAMIC PERFORMANCE OF THE SPIN-WING CONCEPT

Steven K. Tayman and Andrea B. Walden
TEW Division, Vehicle Research Section, Code 5712.2

INTRODUCTION:

The adaptability of unmanned air vehicles (UAV's) to shipboard and remote site operations is of great interest to the Navy. The capability of a single UAV to embody both forward flight (airplane) and hover (helicopter) modes would greatly enhance Navy operations. The helicopter mode would allow flight operations from confined areas. The airplane mode would allow the vehicle to have the speed, range, and endurance required by many missions.

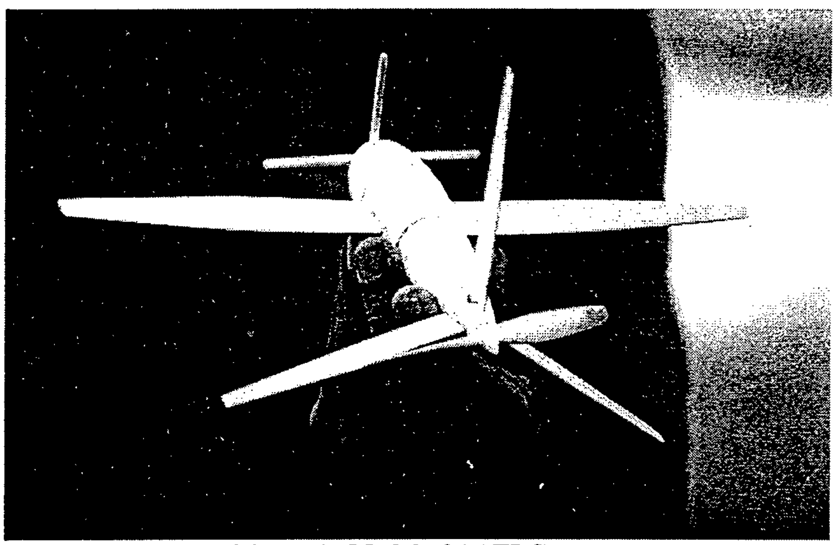

Figure 1. Model of AATI Concept.

The Naval Research Laboratory (NRL) is currently investigating a unique Vertical Take-Off and Landing (VTOL) aircraft concept called the Spin Wing/Stop Rotor developed by Advanced Aerospace Technologies, Inc. (AATI) through an NRL Cooperative Research and Development Agreement (CRADA). A model of this concept (in airplane mode) is pictured in Figure 1. The purpose of this investigation is to analyze the capabilities of the Spin Wing/Stop Rotor concept. AATI has demonstrated a radio-controlled version of the Spin Wing that is capable of transitioning from airplane mode to an autorotative descent and back to airplane mode but is not capable of controlled hovering. This paper focuses on the investigation of the aerodynamic performance in both the helicopter and airplane modes. The example aircraft used to facilitate the analysis is an electric powered, 20-lb, man-portable UAV. A simplified

Manuscript approved January 16, 1998

dynamic computer simulation of the Spin Wing example aircraft was performed to assess the stability and control characteristics of the vehicle in hovering flight. This mode is considered the highest risk flight mode due to the relatively low tip speeds, low disk loading, and unique geometry associated with the Spin-Wing concept.

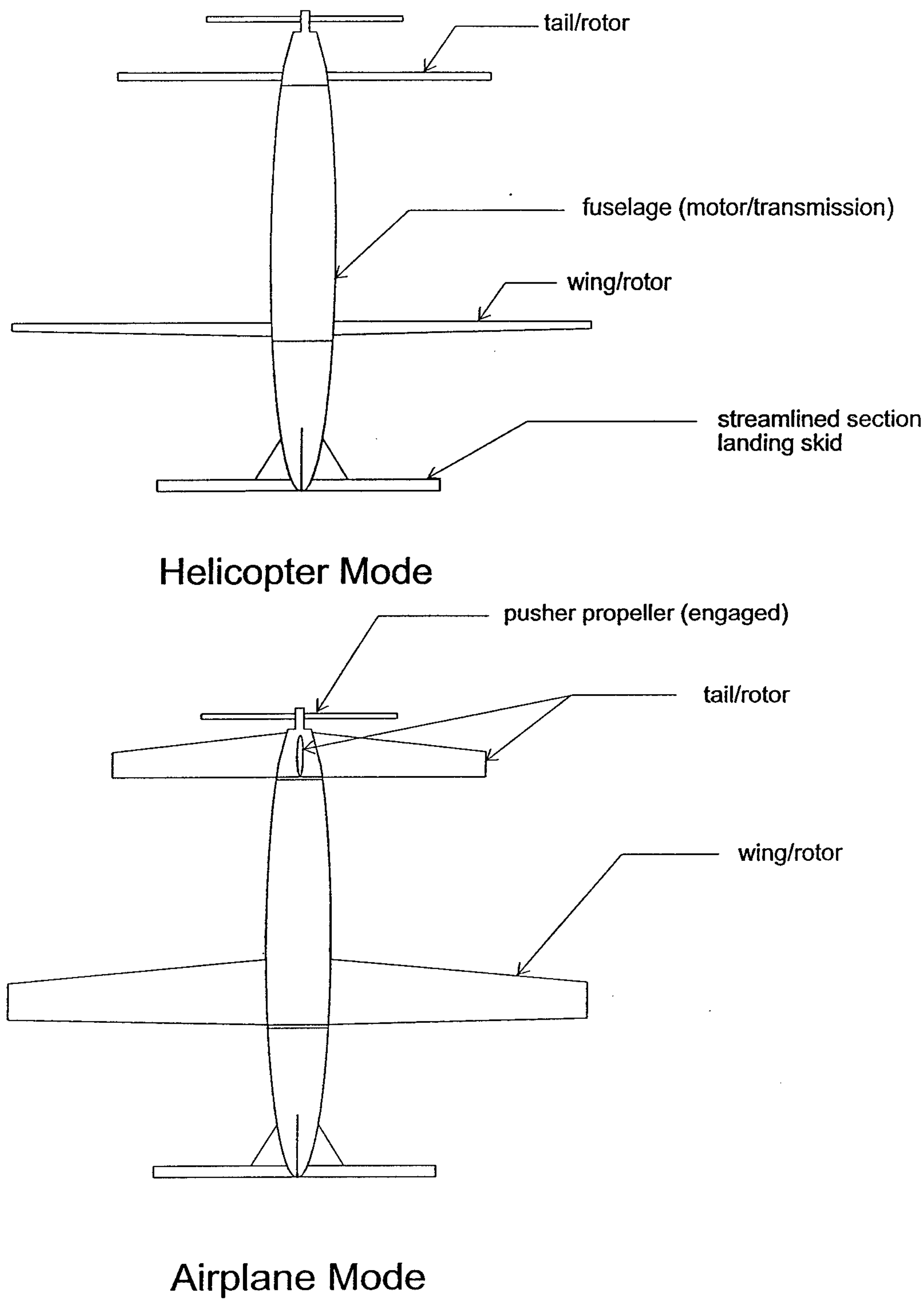

Figure 2. AATI Concept and Primary Component Definitions.

The Spin-Wing/Stop-Rotor concept provided by AATI and the primary component definitions are pictured in Figure 2. The flight profile of the vehicle is depicted in Figure 3. During helicopter mode, the vehicle hovers with its "aircraft" nose down. Both the wing and the tail rotate approximately 90 degrees in pitch at the fuselage juncture and behave as counter-rotating rotors. The tail is driven by a motor/transmission which rotates with the wing. The torque transmitted to the tail is therefore equal and opposite to the torque transmitted to the wing. The yaw of the nose would be controlled by a small electric motor and gear drive. The yaw position of the nose determines the cyclic control orientation, i.e. which way is forward in hover. The tail consists of three blades/surfaces to provide both directional and longitudinal stability in forward flight or airplane mode. The propeller is disengaged from the transmission in the helicopter mode and is allowed to windmill. During the airplane mode, the wing and tail rotate back to their normal positions and function as both a fixed wing with variable incidence control and a horizontal/vertical tail. The tail would be disengaged from the transmission and the pusher propeller engaged to provide thrust in forward flight. In order to convert to airplane mode, the vehicle is required to perform a transition dive from the helicopter mode to its forward flight speed. The vehicle converts back to helicopter mode by decelerating to its minimum speed. Once this minimum speed is attained, the pitch or angle of the wing/rotor with respect to the freestream velocity rapidly changes. This change in pitch causes the wing/rotor to autorotate. The vehicle pitches nose down when the wing/rotor is spun up and the tail/rotor is still in the airplane mode position. Power from the propeller is shifted to the tail/rotor after the tail/rotor pitch is changed to helicopter mode position. Soon afterward, the vehicle transitions from its autorotative descent to steady state hover. The vehicle lands in this mode. Aerodynamically shaped skids are used on the vehicle for stability during take-off and landing.

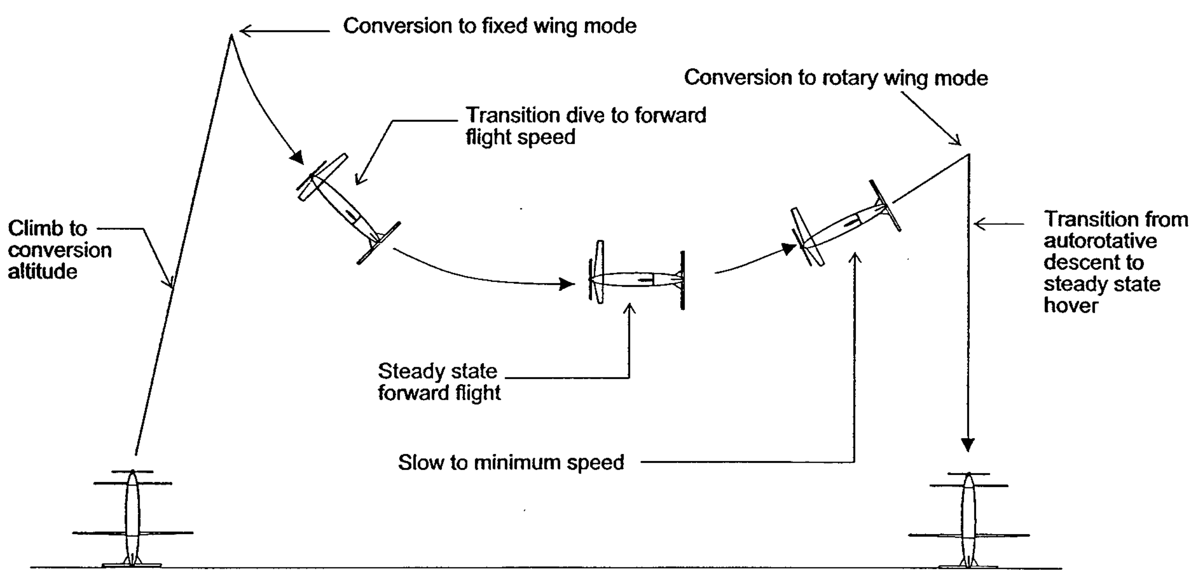

Figure 3. Flight Profile of AATI Concept.

PRELIMINARY SIZING:

In order to facilitate the performance analysis of the Spin-Wing concept, an example aircraft was selected. The example aircraft is a man portable UAV with a weight of 20 lbs. It would be powered by an electric motor with lithium batteries and have a 5 lb payload capability. A loiter speed (minimum power required) of 45 mph (66.2 fps) was chosen to obtain reasonable endurance based on NRL's experience with an electric aircraft of this size. From this velocity, the dynamic pressure, q, was calculated to be approximately 5.2 psf, where q is defined as:

$$q = \frac{1}{2}\rho V^2 \tag{1}$$

where ρ is the density of air, and V is the vehicle velocity. The vehicle would be somewhat similar to the Pointer UAV, a 10 pound, hand-launched reconnaissance vehicle manufactured by AeroVironment, Inc. Being man portable, the maximum wingspan that was considered for the Spin-Wing vehicle was 8 feet.

Because the wing is used for both forward flight and hover there is a close relationship between loiter speed and hover tip speed. If a slow (low power) loiter is desired, the tip speed in hover with the wing/rotor at optimum pitch is also low. Unfortunately, low tip speeds restrict the helicopter-mode-maximum-forward flight speed and most importantly, the ability to hover in high winds. A forward flight speed capability of 30 mph was chosen as an optimum, allowing operations on most days and maintaining a low power requirement for hover. If the maximum advance ratio is conservatively assumed to be 0.35, then the minimum tip speed is 85.7 mph (126 fps).

The example aircraft defines two important parameters, the wing loading and the power available for hover. The wing loading, W/S is defined as:

$$\frac{W}{S_W} = \frac{q}{C_L} \tag{2}$$

Assuming a wing lift coefficient, C_L of 1.0 for loiter in the airplane mode, the wing loading for standard sea level conditions would be approximately 5.2 psf. Typical lithium batteries, utilized by NRL, have a power density of approximately 90 W/lb. Assuming that the battery weight is 1/3 of the vehicle weight (6.67 lbs), the available battery power is 600 W. This assumption provides approximately 480 W of shaft power at the rotors assuming a combined motor/transmission efficiency of 80%. Based on these considerations and allowing some climb margin, the maximum hover shaft power available was considered to be 420 W.

With the wing loading set at 5.2 psf to meet the loiter speed requirement of 45 mph, and a weight of 20 lbs, a resulting wing area, S_W, of 3.85 sq ft is obtained. Once the wing area was determined, the aspect ratio which is defined as:

$$AR_W = \frac{{b_W}^2}{S_W} \tag{3}$$

can be obtained as a function of wingspan, b_W, i.e., a wingspan of 6 feet requires an aspect ratio of 9.36. It was also decided that a wing taper ratio of 0.5 would be fixed for a large portion of the analysis. The requirement for a symmetrical airfoil for the wing and tail led to the choice of the NACA 0012 due to the large availability of data. Since the wing/rotor cannot have twist due to the asymmetry this would cause in airplane mode, it was assumed that the wing/rotor has no twist. In another effort to simplify the analysis, the tail/rotor also has no twist.

Some important factors that were not directly included in the analysis for simplicity should be mentioned. The effect of design variables on structural weight was not included in the analysis. For the same wing area, a higher aspect ratio wing would typically be somewhat heavier. Finally, the effect of motor/transmission output, revolutions per minute (rpm), on weight and efficiency was not accounted for but should be small for the range of rpm's considered for the example aircraft.

COMPUTATIONAL METHOD:

A combined blade element and momentum approach was adopted as the method used to compute the aerodynamic forces acting on the wing/rotor and tail/rotor in hover. The downwash for each rotor is modeled as independent discrete annulus elements. Blade element lift and drag forces are calculated for each annulus element using 2-D data for the NACA 0012 airfoil. This method is computationally straightforward, captures the basic physics of the situation and is generally considered adequate for performance estimates. Several assumptions were used in the computations. First, the center of gravity (CG) is assumed to be located at the aerodynamic center of the wing/rotor and that the feathering axis of the wing/rotor is at its aerodynamic center. Secondly, it is assumed the tail/rotor inflow is independent of the wing/rotor. When air flows through a rotor, the outflow diameter narrows or contracts downstream reaching an equilibrium state. It is assumed that the outflow or downwash from the tail/rotor during hover is fully contracted before it hits the wing/rotor. According to Johnson[1], a wake is fully contracted at a downstream distance greater or equal to ½ times the diameter of the rotor. It is therefore assumed that the distance between the tail and wing is greater than or equal to the radius of the tail/rotor. At this distance, the induced velocity doubles from that of the wake at the trailing edge of the rotor. Momentum continuity therefore dictates the contracted wake to have ½ the area of the initial wake. The tail/rotor downwash is super-imposed on the wing/rotor inflow by contracting each annulus element of

downwash from the tail/rotor. The effect of the fully contracted downwash of the tail/rotor on the wing/rotor is illustrated in Figure 4.

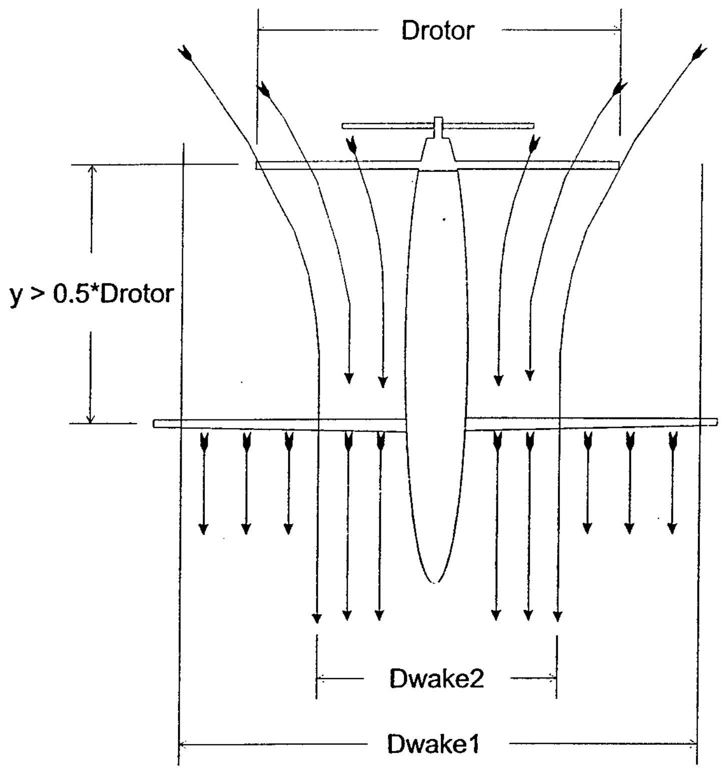

Figure 4. Effect of Tail/Rotor Downwash on Wing/Rotor During Hover.

During the computational process, it is presumed that the combined thrust always equates to the weight during hover. As required for trim, the tail/rotor torque also has the same value as the wing/rotor torque. Another important variable is the thrust weighted lift coefficient, which is defined as:

$$\overline{C_L} = \frac{\int_0^R c_l(r) \times dT}{\int_0^R dT} \qquad (4)$$

where dT is defined as the incremental thrust, r is the distance to the blade element from the center of rotation, and c_l is the local lift coefficient of the blade element. Conventional helicopters in hover at standard sea level conditions usually have thrust weighted lift coefficients ($\overline{C_L}$) between 0.3 and 0.6. The higher the $\overline{C_L}$, the more efficient the vehicle is in hover up to near stall of the blade airfoil; however, this is not practical due to the

considerations of hovering at altitude and maneuvering which require some margin with respect to stall.

The vehicle fuselage size was estimated after reviewing previously developed NRL UAV's and considering the battery volume and motor/transmission required. The fuselage maximum diameter was assumed to be 0.5 feet.

Once these values were prescribed, the combined blade element and momentum approach was used to obtain the rotational speed of the tail/rotor and wing/rotor, and the pitch of the tail/rotor and wing/rotor which corresponded to hover trim. The method is as follows:

1. The geometry of aircraft is defined and an initial estimate for trim is set.
2. The forces on the tail/rotor are integrated radially.
3. The induced velocity produced by the tail/rotor is calculated.
4. The downwash of the tail/rotor on the wing/rotor is computed.
5. The forces on the wing/rotor are then integrated radially.
6. A Newton-Raphson[2] based numerical iterative technique is used to solve for the changes required in the control variables such as the pitch of the wing and tail to converge to a trimmed hover flight solution.
7. Forward-flight loiter performance for this geometry is then estimated.

Forward-flight loiter performance was estimated by assuming that the CG was at the wing aerodynamic center and that the tail carried no lift load. This should be conservative because the tail provides more than enough stability because it has an area that is close to 70% of the wing and a moment arm of at least 32% the wingspan. The wing lift and drag was estimated using the classical induced drag formula for a loiter lift coefficient (C_L) of 1.0. For estimating forward flight performance, a drag coefficient of the body (C_D) was roughly estimated to be about 0.1 after reviewing Prouty[3], who presented drag values from aircraft and helicopter fuselages at zero lift. No additional drag due to the landing skids or interference drag was included. Propeller efficiency was assumed to be 75%. Because of the simplifications applied to the forward flight performance estimates, it is intended only as a rough estimate to allow the examination of trends due to design changes and to illustrate the basic level of performance possible with the Spin-Wing concept.

RESULTS:

The first design problem focused on the effect of the geometry of the tail/rotor relative to the wing/rotor on hover performance. A very useful simplification of the problem was to assume that the tip speeds of the two rotors are equal in hover. If there were significant differences in tip speeds between the two rotors, the rotor with the lowest

tip speed would limit the translational flight speed. Also, since profile power required for a rotor is roughly proportional to the cube of the tip speed; any mismatch in tip speed is likely to increase power required. Since the minimum tip speed has been determined, the only option is to allow the tail/rotor tip speed to be greater than the wing/rotor. This, however, seems unlikely to provide any performance benefit. Therefore, it was decided that for most of this analysis, the tip speed of the tail/rotor should be equal to the wing/rotor.

With the rotor tip speed set at 126 fps, and the taper ratio set at 0.5, the remaining two variables that need to be set are the tail span and tail area. Another key assumption is that the rotor thrust weighted lift coefficients of the tail/rotor should be equal to that of the wing/rotor. This assumption seems reasonable so that the rotors are well matched for stability and control considerations. However, as will be presented later, there is a performance benefit derived from pushing the tail/rotor hover C_L higher than the wing for both hover and forward flight. The computer program generated trimmed hover flight solutions given all of the assumptions discussed to this point for a given wingspan with various tail spans. Geometric definitions for the vehicle are illustrated in Figure 5.

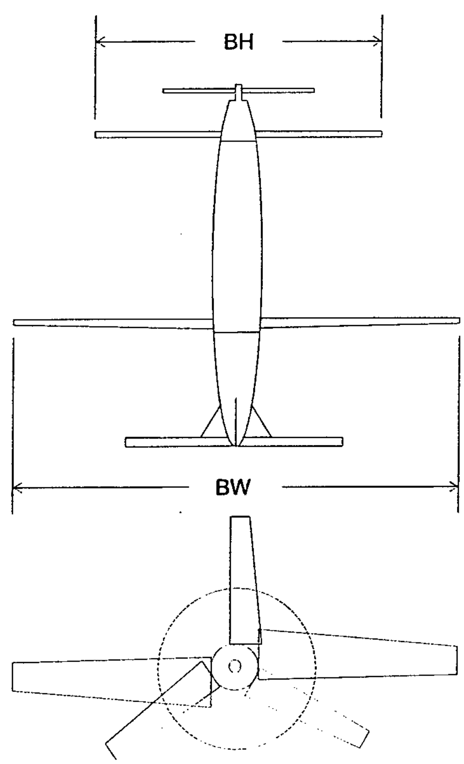

Figure 5. Geometric Definitions for AATI Concept.

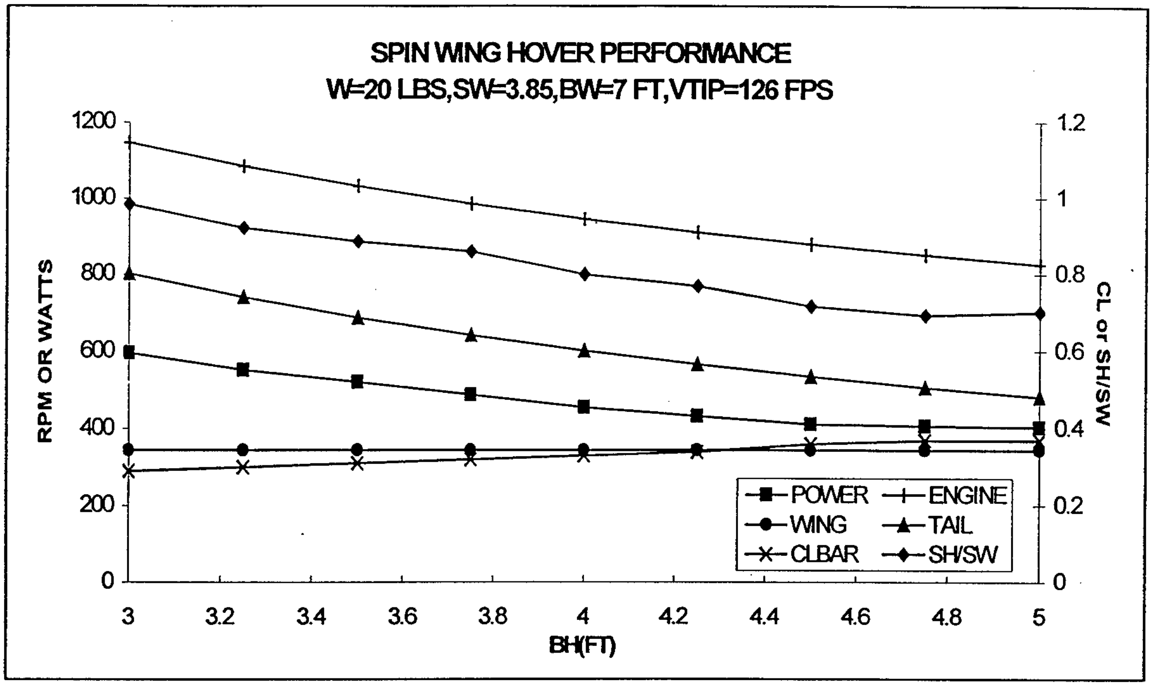

Figure 6. Various Computed Parameters as a Function of Tail Span.

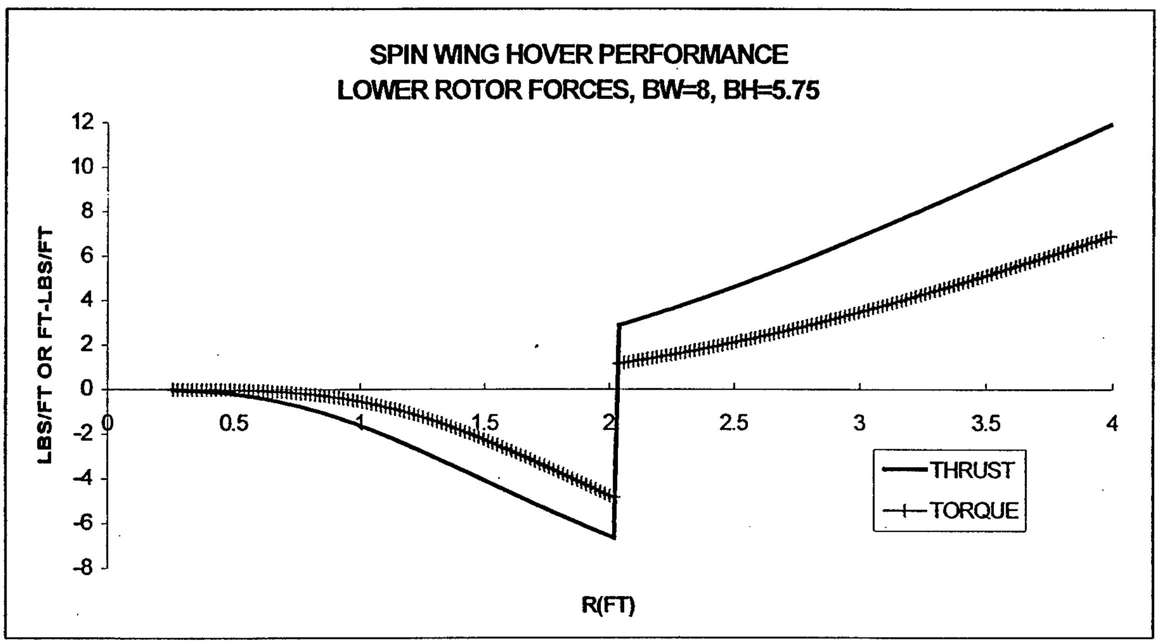

Figure 7. Wing/Rotor Forces.

Figure 6 depicts the power required, rotor rpm, motor rpm, wing C_L, and tail area ratio for a wingspan of 7 feet and tail spans varying from 3 to 5 feet. As would be expected, power required decreased with increasing tail span. However, at about 4.5 feet, the curve becomes very flat. For structural reasons, it is desirable to keep the tail aspect ratio as small as possible. Therefore, the optimum design for hover performance seems to occur

for a tail span of 4.5 feet which corresponds to a tail/wing area ratio of about 0.700 and an aspect ratio close to that of the wing/rotor. There are two fundamental limitations on the effectiveness of larger tail/rotors: 1) the torque is equal between the wing and tail, and 2) the downwash of the tail/rotor generates a download on the wing/rotor. In fact it is interesting to note that in addition to a download, the tail/rotor downwash also generates a negative torque load as illustrated in Figure 7. This negative torque of the inner portion helps offset the download by driving the positively loaded outer portion of the wing/rotor.

In airplane mode, the area of the tail is assumed only to affect the profile drag of the aircraft and therefore has a fairly small effect on loiter power required. Because the hover power is the limiting condition for the example aircraft, improving the loiter performance by decreasing the area of the tail was not examined. However, this may be a reasonable option for other missions where hover power is not so limited. Matching the rotor tip speeds, however, would lead to very high aspect ratio tail surfaces. Another option is to abandon tip speed matching, and allow the tip speed of the tail/rotor to be higher than the wing/rotor with the consequence of higher power required in hover since the minimum allowable tip speed would still apply to the wing/rotor.

The next design problem focused on defining the wingspan. With wing area fixed, the wingspan sets the aspect ratio as exhibited by Equation 3. Fixing the tail/wing area ratio at 0.700 and the tail/wingspan ratio at 0.642, the computer program was used to generate performance results as a function of wingspan. The power required for both hover and forward flight is graphed in Figure 8 with respect to B_W. As would be expected, the vehicle with a larger wingspan requires lower power in hover and forward flight. However, larger wingspans demand higher structural weights due to a higher aspect ratio. It should be considered that for the example aircraft, the choice of a 7-foot wing would be the minimum wingspan that could meet the 420 W hover power requirement with little margin. The loiter lift-to-drag ratio is estimated to be about 15:1. With a loiter power required of only 180 W and an available battery energy of 530 W-hrs, the example aircraft could have a duration of over 2 hours if the combined weight of the structure and flight control system could be kept to about 6 lbs. Fully examining performance considerations, it appears feasible to develop a Spin-Wing UAV which can operate on the limited power density of currently available lithium sulfur-dioxide batteries. This would be difficult to achieve with any other VTOL concept (except a pure helicopter) considering the relatively low power available for hover.

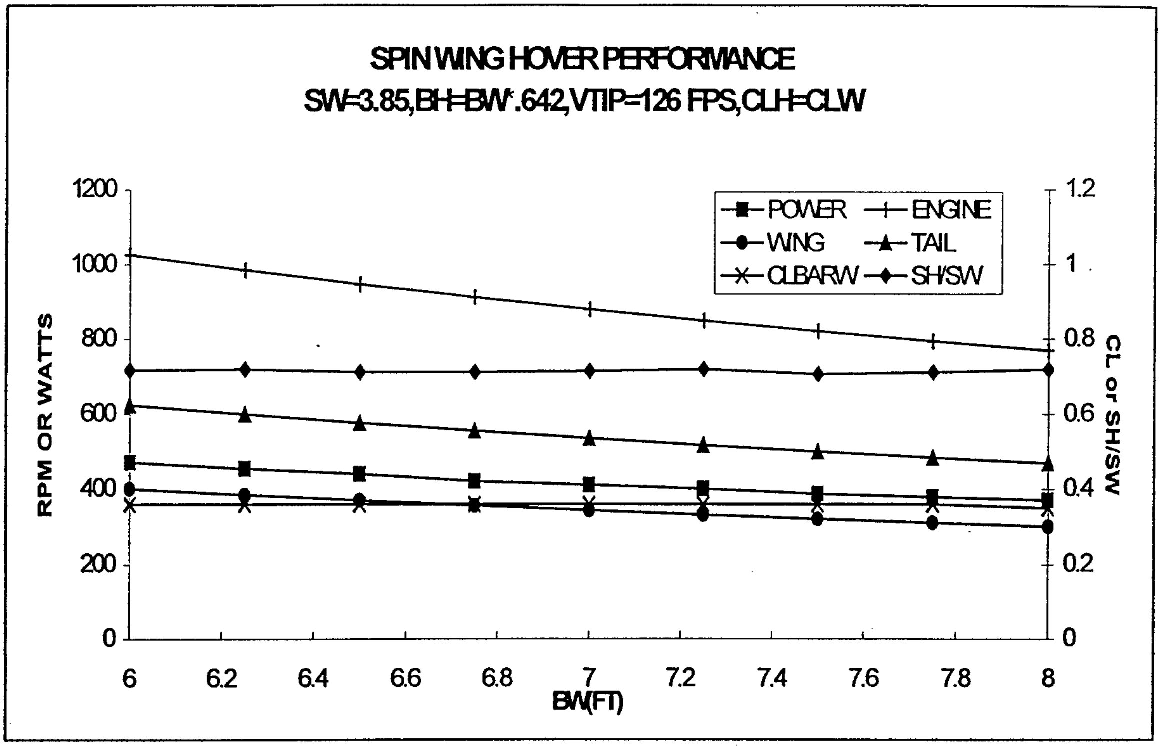

Figure 8. Computed Parameters for Both Hover and Forward Flight as a Function of Wingspan.

Another performance advantage of the Spin Wing as a VTOL aircraft is that its minimum power required in airplane mode occurs at a high flight speed relative to an equivalent helicopter or very high equivalent advance ratio (about 0.53 for the example aircraft). This means that the aircraft can cover more ground and be less sensitive to winds while loitering. Other advantages are the superior range and higher cruise speed compared to an equivalent helicopter. With a lift-to-drag ratio of 15:1, the range should be more than double that of an equivalent helicopter and occur at a much higher flight speed. The maximum speed obtained from a hover power of 420W is approximately 81.6 mph (120 fps), which is equivalent to an advance ratio of 0.95. A detailed comparison with other VTOL concepts for UAV's such as the Tiltrotor and Heliwing are beyond the scope of this report, but it seems clear that the Spin Wing offers the potential for some significant performance advantages.

CONCLUSION:

This report has discussed some of the unique performance characteristics of the Spin Wing in hover and low speed forward flight. One interesting design decision is the compromise between wing loading in forward flight and rotor tip speed in hover. Once a hover tip speed is chosen, the only way to decrease the wing loading is to hover at a lower blade lift coefficient which increases hover power required. Because the minimum tip speed is limited for hovering in winds, most designs will have a wing loading in the

moderate to high range which makes the Spin Wing especially suitable for missions requiring high cruise speeds and VTOL capability.

Another interesting design problem is the size and shape of the tail/rotor relative to the wing/rotor. The matching of the wing to the tail in hover was investigated and a tail/rotor diameter equal to 64% the wing/rotor diameter was determined to be close to optimum from a hover performance point of view with the tail/rotor blade area equal to 70% of the wing area. The tail/rotor aspect ratio is roughly equal to that of the wing/rotor.

The Spin Wing offers the potential for exceptionally low power required in hover and a good lift-to-drag ratio in forward flight. From a performance point of view, this seems to compare very favorably with other VTOL designs such as the Tiltrotor. The vehicle is very aerodynamically clean in airplane mode and has a very large rotor for efficient hover. Even though the inner portion of the wing/rotor carries a very heavy download from the downwash of the tail/rotor, the negative autorotation torque load greatly compensates for this and the overall penalty appears to be quite modest using the combined momentum blade element theory.

Potential problem areas for the Spin Wing include the free-fall transition to forward flight, and the weight and complexity of the flight control system to allow both hovering and airplane flight. Both rotors will require collective control with a very large range of travel. The conditions that the nose is the reference for control inputs and that the engine/transmission rotates with the wing require signals and/or power to pass between rotating bodies. This adds weight and complexity to the vehicle. The Spin Wing may also have vibration problems in hover due to the very rigid two-bladed wing/rotor. Most helicopters with stiff blade suspensions have three or more blades. A simplified dynamic computer simulation of the Spin-Wing example aircraft demonstrated that stability augmentation using rate gyros in all three axes would be required for acceptable stability and control characteristics in hover. Although the development of a Spin-Wing vehicle introduces many mechanical design challenges, the Spin-Wing concept offers the potential for an excellent compromise between hover and high-speed flight. The Spin-Wing concept therefore deserves further investigation as potential technology to address Navy requirements and needs.

ACKNOWLEDGMENTS:

The authors would like to thank the Office of Naval Research (ONR) ECM Development Technology for sponsoring the CRADA with AATI. Also many thanks to Randy McDonnell, President of AATI, for his many useful insights and suggestions during the performance analysis of the Spin-Wing concept which he originated.

REFERENCES:

[1]Johnson, W., *Helicopter Theory*, Dover Publications, Inc., New York, 1980, p. 119.

[2]Prouty, R.W., *Helicopter Performance, Stability and Control,* Robert E. Krieger Publishing Company, Malabar, Florida, 1990.

[3]Anderson, D.A., Tannehill, J.C., and Pletcher, R.H., *Computational Fluid Mechanics and Heat Transfer*, Taylor & Francis, 1984, p.369.

NOMENCLATURE

AR_w	Aspect ratio of wing/rotor
AR_H	Aspect ratio of tail/rotor ($AR_H = 1.5 \times [B_H^2/S_H]$)
B_H	Span of tail/rotor
B_W	Span of wing/rotor
C_D	Drag coefficient
CG	Center of gravity
c_l	Local lift coefficient
C_L	Lift coefficient
$\overline{C_L}$	Thrust weighted lift coefficient (CLBAR)
CL_H	Tail/rotor lift coefficient
CL_W	Wing/rotor lift coefficient
Drotor	Rotor diameter
dT	Incremental thrust
Dwake1	Initial full wake diameter
Dwake2	Fully contracted wake diameter
ρ	Air density
r	Radial distance to blade element
SH	Tail/rotor area
SW	Wing/rotor area
Vtip	Blade tip velocity
y	Vertical distance between tail/rotor and wing/rotor

fps	Feet per second
psf	Pounds per square foot
mph	Miles per hour
W	Watts

AATI	Advanced Aerospace Technologies, Incorporated
CRADA	Cooperative Research and Development Agreement
NACA	National Advisory Committee for Aeronautics
NRL	Naval Research Laboratory
UAV	Unmanned air vehicle
VTOL	Vertical take-off and landing